Journal of Statistical Physics, Vol. 77, Nos. 3/4, 1994

Two Repulsive Lines on Disordered Lattices

Lei-Han Tang[1]

Received March 4, 1994

We investigate the ground-state properties of two lines with "on-site" repulsion on disordered Cayley tree and (Berker) hierarchical lattices, in connection with the question of multiple "pure states" for the corresponding one-line problem. Exact recursion relations for the distribution of ground-state energies and of the overlaps are derived. Based on a numerical study of the recursion relations, we establish that the total interaction energy on average is asymptotically proportional to the width δ of the ground-state energy fluctuation of a single line for both weak and strong (i.e., hard-core) repulsion. When the length t of the lines is finite, there is a finite probability of order t^{-a} for (nearly) degenerate, non-overlapping one-line ground-state configurations, in which case the interaction energy vanishes. We show that $a = \omega$ ($\delta \sim t^{\omega}$) on hierarchical lattices. Monte Carlo transfer matrix calculation on a $(1+1)$-dimensional model yields the same scaling for the interaction energy but an a different from $\omega = 1/3$. Finite-length scalings of the distribution of the interaction energy and of the overlap are also discussed.

KEY WORDS: Directed polymer; disorder; hierarchical lattice; overlap; rare event; replica.

1. INTRODUCTION

The problem of directed lines (also known as directed polymers) in a disordered potential has been a subject of recent interest due to its application to flux-line pinning in high-T_c superconductors[1-4] and due to its fundamental role in the theory of disordered systems.[5-10] A prototype system is that of two lines with a short-ranged repulsive interaction (see Fig. 1). In a continuum formulation, the configuration of the two lines is

[1] Institut für Theoretische Physik, Universität zu Köln, D-50937 Köln, Germany. tang@thp.uni-Koeln.de.

822/77/3-4-5

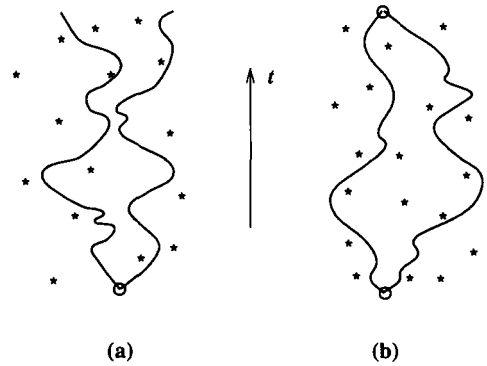

Fig. 1. Two directed lines in a disordered medium with (a) one common endpoint and (b) two common endpoints.

specified by their transverse displacements $\mathbf{x}_1(t)$ and $\mathbf{x}_2(t)$. The energy of the system is given by

$$H = H_1(\{\mathbf{x}_1\}) + H_2(\{\mathbf{x}_2\}) + H_{\text{int}}(\{\mathbf{x}_1 - \mathbf{x}_2\}) \tag{1.1}$$

where

$$H_1(\{\mathbf{x}\}) = \int dt \left[\frac{K_1}{2} \left(\frac{d\mathbf{x}}{dt} \right)^2 + \varepsilon(\mathbf{x}, t) \right] \tag{1.2a}$$

$$H_2(\{\mathbf{x}\}) = \int dt \left[\frac{K_2}{2} \left(\frac{d\mathbf{x}}{dt} \right)^2 + \varepsilon(\mathbf{x}, t) \right] \tag{1.2b}$$

$$H_{\text{int}}(\{\mathbf{x}\}) = \int dt\, V(\mathbf{x}) \tag{1.2c}$$

Here K_1 and K_2 are the line tensions, $\varepsilon(\mathbf{x}, t)$ is a (e.g., Gaussian) random potential with a short-ranged correlation, and $V(\mathbf{x})$ is the potential for the interaction of the two lines. Typical questions one asks are: (a) do the two lines form a bound state, and (b) how does the excess energy due to interaction vary with the length of the line? etc.

A limiting case of (1.1) is $K_1 = \infty$ and K_2 finite. As line 1 becomes infinitely stiff, it acts as a columnar defect that interacts with line 2 through the potential V. The latter problem has been examined recently by several groups and a consensus concerning question (a) has emerged.[3,11–13] It is plausible that this case is representative of the general situation $K_1 \neq K_2$, since the ground-state configurations of a single line at different values of K are expected to have little overlap with one another when the line is sufficiently long.

A different situation arises when the two lines are equally flexible, i.e., $K_1 = K_2$. Due to the presence of disorder, it is not possible to reduce this case to that of one line in a columnar potential using relative coordinates. The fact that the ground state of (1.2a) is also the ground state of (1.2b) introduces an effective attraction between two lines which then compete with the repulsive part (1.2c). (This effect is manifest in replica treatment of the problem; see refs. 1, 3, and 7.) From the properties of the one-line ground-state, Parisi[8] and Mézard[9] proposed three possible scenarios in the case of a weak repulsion:

(i) There is a single deep valley of the energy functional (1.2a) where the ground state lies. The two lines form a bound state in the valley, with an excess energy $E_{\text{int}} \sim t$, where t is the length of the line.

(ii) The energy functional (1.2a) has multiple deep minima which are almost degenerate but well separated from each other. This corresponds to "replica symmetry breaking." The formal attraction disappears, and the two lines go to different valleys. The excess energy $E_{\text{int}} = O(1)$ as $t \to \infty$.

(iii) The energy functional (1.2a) has multiple deep minima, but the energy gap between them grows as $t^{\tilde{\omega}}$. Thus only a single valley is thermodynamically accessible, but other valleys are relevant for the two-line problem. In particular, when the lines are sufficiently long, they minimize their overlap by going to different valleys, giving rise to an excess energy $E_{\text{int}} \sim t^{\tilde{\omega}}$.

The calculations performed by Parisi and Mézard in $(1+1)$ dimensions suggest that (iii) is most likely the case, but (ii) occurs occasionally, with a probability of order t^{-a}. This rare event is not quite sufficient to produce a broad distribution of overlaps which is typical for spin-glasses, but would dominate the response to an applied transverse field when $a = \omega$, where ω is the energy fluctuation exponent.[9,10] For two repulsive lines, the above picture leads to the expectation that any small but finite interaction is able to drive them apart, and that the increase in the total energy is of order $t^{\tilde{\omega}}$. Numerical simulations by Mézard suggest that, in $(1+1)$ dimensions, $\tilde{\omega} = \omega = 1/3$.

In this paper we investigate the ground-state of a system of two repulsive lines on the Cayley tree (Fig. 2(a) and on the (Berker) hierarchical lattices (Fig. 2b) with disorder. The advantages of these lattices is that exact recursion relations for quantities of interest can be derived and iterated numerically to any desired accuracy.[5,14] Here we shall focus on the distribution of the excess energy E_{int} in the ground state of the two-line system, and the distribution of the overlap of (nearly) degenerate ground states of the one-line system. Our results in general support and further quantify the picture proposed by Parisi and Mézard for the $(1+1)$-dimen-

sional case. As a comparison, we present in addition some Monte Carlo transfer matrix results for two lines on a $(1+1)$-dimensional lattice with hard-core repulsion. Surprisingly, we found in this case $a = \zeta = 2/3$.

Hierarchical lattices are often thought of as approximations to finite-dimensional lattice on which the Migdal–Kadanoff transformation becomes exact.[15] Here we would like to emphasize a new perspective in relating hierarchical lattices to the finite-dimensional ones when the object under consideration, i.e., a directed line, is spatially extended and intrinsically anisotropic. Roughly speaking, one can view a hierarchical lattice as arising from a partition of a finite-dimensional regular lattice in such a way that the number of branches b is the same (in a statistical sense) as the number of independent competing paths in real space on a given scale. Obviously this number depends on the dimensionality of the regular lattice and also on the transverse fluctuations of the line (i.e., the region "seen" by the line), but a precise relation is not known. (Otherwise we would have solved the problem!) On the hierarchical lattice, the branching and competition occur on all levels, mimicking scale invariance in real space. Thus, from a phenomenological point of view, the basic physics of a directed polymer in a d-dimensional disordered medium is captured by the corresponding model on the hierarchical lattice, although we do not know how b is related to d. Following a similar line of thought, it is reasonable to expect that the problem of two interacting lines with the two pairs of ends tied together (see Fig. 1b) can be faithfully represented on the hierarchical lattice, which will be specified in detail below.

The paper is organized as follows. In Section 2 we introduce the model and derive recursion relations for the distribution of the ground-state energies and of the overlaps. Section 3 presents results of a numerical investigation of the recursion relations on the Cayley tree. Results on the hierarchical lattices are discussed in Section 4. In Section 5 we discuss results of a Monte Carlo transfer matrix calculation in $(i+1)$ dimensions. Section 6 contains a summary of main findings of the paper. An approximate calculation of the ground-state energy of a single line on the Cayley tree using rare-event statistics is presented in the appendix.

2. THE MODEL AND RECURSION RELATIONS

2.1. The Model

Let us first recall the problem of a single directed line on the Cayley tree with disorder.[5] The tree is arranged hierarchically as shown in Fig. 2a, with the root on top and symmetric twofold branching at every integer distance from O. The allowed configurations of the line are no-

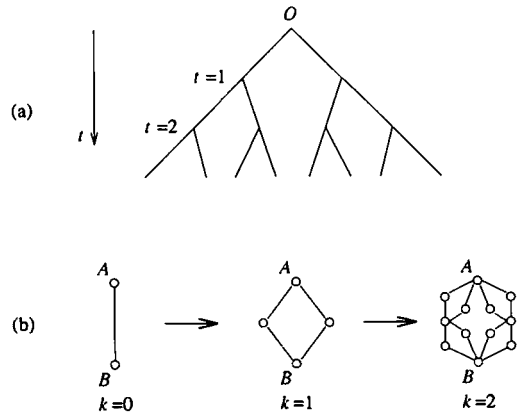

Fig. 2. (a) The Cayley tree with twofold branching at every integer distance from the root O. A directed line takes a no-return path from the root to any of the bottom branches. (b) The (Berker) hierarchical lattice at $b = 2$. A directed line takes a no-return path from A to B.

return paths that join the root and any of the bottom branches. To each bond on the tree, one assigns a random energy ε whose distribution is given by $\rho_\varepsilon(x)$. The energy of a path is simply the sum of the energy of bonds on that path.

A similar model has been introduced by Derrida and Griffiths on the (Berker) hierarchical lattice.[14] The hierarchical lattice is defined iteratively. Upon each iteration a bond is split into b branches, with two linked bonds on each branch. The case $b = 2$ is shown in Fig. 2b. A directed line is a no-return path that joins the upper and lower ends of the lattice. The number of bonds on such a path at generation k is $t = 2^k$. The energy of a path is given by the sum of random bond energies "seen" by the path.

For the problem of two lines, the allowed configurations for each line are the same as above. The total energy of the system is the sum of bond energies of each line plus an interaction energy. Here we consider only a contact interaction. When two lines share a given bond, there is an interaction energy V. For reasons which will become clear later, we take V to be a quenched random variable with a distribution $\rho_V(x)$. The total interaction energy is the sum of the interaction energies on shared bonds.

One can introduce a slightly more general model by considering still the same set of line configurations but a different way of assigning the energy to a given configuration. The energy of a bond is a function of the number of lines n that go through it,

$$\varepsilon_B(n) = \varepsilon\delta_{n,1} + \tau\delta_{n,2} \tag{2.1}$$

Here ε and τ are quenched random variables with a joint probability distribution $\rho(\varepsilon, \tau)$ which may or may not factorize. In the special case defined above we have $\tau = 2\varepsilon + V$ and hence

$$\rho(\varepsilon, \tau) = \rho_\varepsilon(\varepsilon)\, \rho_V(\tau - 2\varepsilon) \tag{2.2}$$

The total energy of the system is the sum of all bond energies ε_B. In this paper we shall consider exclusively nonattractive interactions, for which

$$\rho(x, y < 2x) \equiv 0 \tag{2.3}$$

A remark on notation. For quantities that depend on the length t of the line, we shall use t as a subscript on a Cayley tree, but the lattice generation k ($t = 2^k$) as a subscript on the hierarchical lattices. The subscript is sometimes omitted when all quantities in an equation have the same index.

2.2. Ground-State Energy Distribution

Consider the Cayley tree as shown in Fig. 2a up to a distance t. Let $E_t^{(n)}$ be the ground-state energy of n-lines on the tree, $n = 1, 2$. Noting that the tree can be decomposed into two subtrees of length $t-1$, each with an additional bond attached to the top, one may write

$$E_t^{(1)} = \min\{E_{t-1}^{(1)} + \varepsilon,\ E_{t-1}'^{(1)} + \varepsilon'\} \tag{2.4a}$$

$$E_t^{(2)} = \min\{E_{t-1}^{(2)} + \tau,\ E_{t-1}'^{(2)} + \tau',\ E_{t-1}^{(1)} + \varepsilon + E_{t-1}'^{(1)} + \varepsilon'\} \tag{2.4b}$$

Here unprimed and primed quantities on the right-hand side of (2.4) refer to the left and right branches of the tree, respectively. For nonattractive interaction we have, in a given realization of disorder,

$$E_t^{(2)} \geqslant 2E_t^{(1)} \tag{2.5}$$

Derrida and Griffiths[14] have shown that a simple way to analyze the one-line problem defined by Eq. (2.4a) is to introduce a probability distribution for the ground-state energy, for which a recursion relation can be obtained. In our case, $E^{(1)}$ and $E^{(2)}$ on the same tree are correlated. It is thus necessary to consider the joint probabilities

$$P_t(x, y) \equiv \text{Prob}\{E_t^{(1)} \geqslant x \text{ and } E_t^{(2)} \geqslant y\} \tag{2.6a}$$

$$Q_t(x, y) \equiv \text{Prob}\{E_{t-1}^{(1)} + \varepsilon \geqslant x \text{ and } E_{t-1}^{(2)} + \tau \geqslant y\} \tag{2.6b}$$

From Eq. (2.5) it follows that

$$P(x, y<2x) = P(x, 2x) \tag{2.7a}$$

$$Q(x, y<2x) = Q(x, 2x) \tag{2.7b}$$

It is easy to see that Q_t can be expressed in terms of P_{t-1} and ρ as

$$Q_t(x, y) = \int dx_1\, dy_1\, \rho(x_1, y_1)\, P_{t-1}(x-x_1, y-y_1) \tag{2.8a}$$

The remaining task is to relate P_t with Q_t to complete the set of recursion relations. This is done below.

Consider the inequalities on the right-hand side of (2.6a). Due to Eq. (2.7a), one only needs to focus on the case $y \geqslant 2x$. To fulfill the inequalities, it is necessary and sufficient that (i) $E^{(1)}_{t-1} + \varepsilon \geqslant y/2$ and $E'^{(1)}_{t-1} + \varepsilon' \geqslant y/2$, or (ii) $x \leqslant E^{(1)}_{t-1} + \varepsilon < y/2$, $E^{(2)}_{t-1} + \tau \geqslant y$, and $E^{(1)}_{t-1} + \varepsilon + E'^{(1)}_{t-1} + \varepsilon' \geqslant y$ simultaneously, or (iii) $x \leqslant E'^{(1)}_{t-1} + \varepsilon' < y/2$, $E'^{(2)}_{t-1} + \tau' \geqslant y$, and $E^{(1)}_{t-1} + \varepsilon + E'^{(1)}_{t-1} + \varepsilon' \geqslant y$ simultaneously. It is easy to convince oneself that the above three situations are mutually exclusive. Hence we have

$$P_t(x, y) = Q_t^2\left(\frac{y}{2}, y\right) + 2\int_x^{y/2-0} dx_1 \left[-\frac{\partial Q_t(x_1, y)}{\partial x_1}\right] Q_t(y-x_1, y) \tag{2.8b}$$

Let us now turn to the minimization problem on the hierarchical lattices. As before, we introduce the joint probabilities for the one- and two-line ground-state energies,

$$P_k(x, y) \equiv \text{Prob}\{E^{(1)}_k \geqslant x \text{ and } E^{(2)}_k \geqslant y\} \tag{2.9a}$$

$$Q_k(x, y) \equiv \text{Prob}\{E^{(1)}_{k-1} + E'^{(1)}_{k-1} \geqslant x \text{ and } E^{(2)}_{k-1} + E'^{(2)}_{k-1} \geqslant y\} \tag{2.9b}$$

Primes indicate a different realization of the bond energies. From the above definition we have

$$Q_k(x, y) = \int dx_1\, dy_1\, \frac{\partial^2 P_{k-1}(x_1, y_1)}{\partial x_1\, \partial y_1}\, P_{k-1}(x-x_1, y-y_1) \tag{2.10a}$$

On the hierarchical lattice of generation k, there are similar relations for the ground-state energies as Eqs. (2.4), except that now each branch consists of two linked lattices of generation $k-1$. Using a similar decomposition of the phase space as done above for the tree, we obtain, for $y \geqslant 2x$,

$$P_k(x, y) = Q_k^b\left(\frac{y}{2}, y\right) + b\int_x^{y/2-0} dx_1 \left[-\frac{\partial Q_k(x_1, y)}{\partial x_1}\right] Q_k(y-x_1, y)^{b-1} \tag{2.10b}$$

At $k=0$, which is the case of a single bond, we have

$$P_0(x, y)=\int_x^\infty dx_1 \int_y^\infty dy_1\, \rho(x_1, y_1) \tag{2.11}$$

2.3. Overlaps

We consider here only the overlap of two noninteracting lines. We shall use s for the number of bonds shared by the two lines in the ground state and $\pi(s)$ for the distribution of s. When the ground state is nondegenerate, we have $s=t$ (full overlap). In the case of a degenerate ground state, the two lines can take different configurations, so that $s<t$. As a convention, s in such a case is chosen to be the *smallest* from the set of possible values.

It is not obvious but nevertheless true that s and the one-line ground-state energy $E^{(1)}$ are in general correlated. Thus to obtain $\pi(s)$ one has to consider the joint probability

$$\hat{P}(x; l)=\text{Prob}\{E^{(1)}\geqslant x \text{ and } s\geqslant l\} \tag{2.12}$$

The overlap distribution π is given by

$$\pi(s)=\hat{P}(-\infty; s)-\hat{P}(-\infty; s+1) \tag{2.13}$$

On the Cayley tree, the following recursion relations are seen to hold for $s\geqslant 1$:

$$\hat{Q}_t(x; s)=\int dx_1\, \rho_\varepsilon(x_1)\, \hat{P}_{t-1}(x-x_1; s-1) \tag{2.14a}$$

$$\hat{P}_t(x; s)=2\int_x^\infty dx_1 \left[-\frac{\partial \hat{Q}_t(x_1; s)}{\partial x_1}\right] \hat{Q}_t(x_1+0; 0) \tag{2.14b}$$

Note that $Q_t(x; 0)\equiv Q_t(x; 1)$ on the tree. For $s=0$, (2.14b) is replaced by

$$\hat{P}_t(x; 0)\equiv \hat{P}_t(x)=\hat{Q}_t(x; 0)^2 \tag{2.15}$$

i.e., the relation for the integrated probability $\hat{P}_t(x)$ of $E^{(1)}$ alone.

For two noninteracting lines on the hierarchical lattices, a similar set of recursion relations hold. For $s\geqslant 1$, two lines must be on the same branch and the ground-state energy on this branch must be lower than those on other branches. This leads to the result, for $s\geqslant 1$,

$$\hat{Q}_k(x;s) = -\int dx_1\, \hat{P}_{k-1}(x-x_1;0)\frac{\partial \hat{P}_{k-1}(x_1;s)}{\partial x_1} + \sum_{l=0}^{s-1}\int dx_1 \frac{\partial[\hat{P}_{k-1}(x_1;l+1)-\hat{P}_{k-1}(x_1;l)]}{\partial x_1}\hat{P}_{k-1}(x-x_1;s-l) \tag{2.16a}$$

$$\hat{P}_k(x;s) = b\int_x^\infty dx_1\left[-\frac{\partial \hat{Q}_k(x_1;s)}{\partial x_1}\right]\hat{Q}_k(x_1+0;0)^{b-1} \tag{2.16b}$$

For $s=0$, Eq. (2.16a) still holds (omitting the sum on the right-hand side), while Eq. (2.16b) is replaced by

$$\hat{P}_k(x;0) \equiv \hat{P}_k(x) = \hat{Q}_k(x;0)^b \tag{2.17}$$

Note that $\hat{P}_k(x;s)$ is determined by those $\hat{P}_{k-1}(x;s')$ with $s' \leqslant s$.

2.4. Numerical Procedure

The results presented in the following sections are obtained through numerical iteration of the recursion relations given above. For this purpose we find it convenient to restrict the random bond energy ε and the interaction energy V to a discrete set of values. Specifically, we take

$$\rho_\varepsilon(\varepsilon) = p\delta(\varepsilon-1) + (1-p)\,\delta(\varepsilon) \tag{2.18}$$

i.e., $\varepsilon = 1$ with probability p and $\varepsilon = 0$ with probability $1-p$. Two types of distribution ρ_V for the interaction energy V are considered. The first type is given by

$$\rho_V(V) = r\delta(V-1) + (1-r)\,\delta(V) \tag{2.19}$$

i.e., $V=1$ with probability r and $V=0$ with probability $1-r$. Although V takes only discrete values, the strength of the interaction can be tuned by varying r. The second type is that of hard-core repulsion, where $\rho_V(V)=0$ for any finite V. In both cases, the joint distribution for one-line and two-line energies is given by Eq. (2.2).

As noted by Derrida and Griffiths,[14] a potential problem associated with distribution of the type (2.18) is that bonds with the lowest energy (0 in this case) percolate on the lattice. When this happens, the minimization problem becomes qualitatively different. In our model, percolation takes place when the probability p for having a high-energy bond becomes

less than a threshold value p_c. On the Cayley tree, $p_{cv} = 1/2$. On the hierarchical lattice, p_c satisfies

$$p_c = [1 - (1 - p_c)^2]^b \tag{2.20}$$

This threshold is given by $p_c = (3 - \sqrt{5})/2 = 0.3819...$ for $b = 2$, $p_c = 0.6106...$ for $b = 3$, etc. For $b \gg 1$ we have $p_c = 1 - b^{-1} - \frac{1}{2}b^{-2} + O(b^{-3})$. Results presented in this paper are for $p = 0.8$ on Cayley tree and the hierarchical lattice at $b = 2$; $p = 0.9$ on the hierarchical lattice at $b = 4$; and $p = 0.95$ on the hierarchical lattice at $b = 8$.

To implement the recursion relations on computer, one first writes them in a discrete form, which we shall not elaborate here. The maximum of the ground-state energy for a single line is simply the length of the line, and the maximum of the ground-state energy for two lines is twice this value. As the length of the line increases, the memory space needed to code the joint probabilities expands rapidly. It turns out that the probability distribution decays exponentially at the tails. One way to save memory and computer time is to truncate the tails. On the hierarchical lattice, it is sufficient for our purpose to keep the truncation error below 10^{-12}. Double-precision representation is used in the iteration process.

The situation on the Cayley tree is quite different. It turns out that the minimization problem is dominated by rate events. (See discussion in the appendix.) Hence great care much be taken in dealing with the truncation error at the lower end of the distribution. In this case we used REAL*16 representation, which allows for 33–34 effective-digit manipulations.

3. CAYLEY TREE

3.1. Noninteracting Lines

This case has been analyzed in great detail by Derrida and Spohn[5] and by Fisher and Huse.[10] Their main findings for the low-temperature phase many be summarized as follows:

(i) The distribution of the ground-state energy $E_t^{(1)}$ has a finite width and exponentially decaying tails. Specifically, the probability $\hat{P}(x)$ as defined by Eqs. (2.12) and (2.15) approaches a "traveling wave" form at large t,

$$\hat{P}_t(x) = W(x - \gamma_t) \tag{3.1}$$

where

$$\gamma_t \equiv \langle E_t^{(1)} \rangle \simeq e_0 t + C \ln t \tag{3.2}$$

Here and elsewhere $\langle \cdot \rangle$ denotes average over different realizations of the disorder. For $x \to -\infty$, we have

$$1 - W(x) \sim -xe^{\psi x} \tag{3.3}$$

The coefficient e_0 is the ground-state energy per unit length, and C and ψ are positive constants. Equation (3.1) in particular implies that the mean-square deviation of $E_t^{(1)}$ is bounded as $t \to \infty$, in contrast to the problem on the hierarchical lattice at finite b.

(ii) In the limit $t \to \infty$, the overlap $q = s/t$ between the ground-state and the second lowest energy state (which is simply another ground state in case of degeneracy) is either 0 or 1. Fisher and Huse[10] studied the energy difference ΔE between the ground-state and the minimum-energy state which branches off from it at a distance $s \ll t$ from the origin O (see Fig. 2a) and found that $\Delta E \sim s^{1/2}$ and that the probability for $\Delta E = O(1)$ is of the order of $s^{-3/2}$.

For the above statements to hold, the distribution $\rho_\varepsilon(x)$ for the single-bond energy should have a "well-behaved" tail on the $x < 0$ side, as evident from discussions presented in the appendix. This is not a worry in our case. There are, however, a few minor differences introduced by the discreteness of energy levels in our model. First, since x in (3.1) is pitched on integers, the mean-square deviation of the ground-state energy in general exhibits a quasiperiodic oscillation, though e_0, C, and ψ should have well-defined limits as $t \to \infty$. Second, there is a finite probability for ground-state degeneracy, giving rise to incomplete (e.g., zero) overlap at zero temperature. This property of the discrete model is shared by models considered in refs. 5 and 10 if we extend the notion of degeneracy to those states whose energies are within a certain finite range from that of the ground state.

Our numerical investigation of the model defined by (2.18) generally confirms the expected behavior mentioned above. Figure 3 shows the distribution of $E_t^{(1)} - \gamma_t$ for $t = 256$ and 512 (solid circles). The points appear to fall on a single curve, in agreement with (3.1). The left end of the curve is well approximated by

$$W'(x) \simeq -2(\psi x + 1)\, e^{\psi x} \tag{3.4}$$

with $\psi \simeq 2.47$ (shown by dashed line). Also shown in Fig. 3 are the partial probability distributions for $E_t^{(1)} - \gamma_t$ at $s = 0$ (open circles) and $s = t$ (crosses). The case $s = t$ corresponds to a nondegenerate ground state, which has a lower mean energy than the average. Indeed, the lower end of the full distribution is dominated by those with $s \simeq t$. In contrast, the upper end of the distribution is dominated by those with $s \simeq 0$.

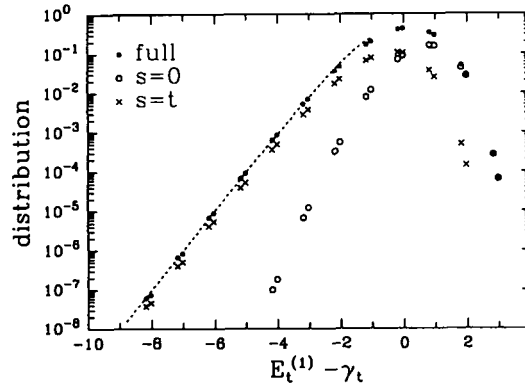

Fig. 3. Distribution of the ground-state energy of a single line on the Cayley tree. Dashed line indicates a fitted curve of the form (3.4).

We have checked that (3.2) describes our data well for $t \geqslant 4$. Plotting γ_t/t against $t^{-1} \ln t$, we obtain $e_0 \simeq 0.253$ and $C \simeq 0.59$. The values for e_0 and ψ agree well with the calculation presented in the appendix, which yields $e_0 = 0.25298...$ and $\psi = 2.469...$ at $p = 0.8$. The amplitude of the logarithmic correction C, however, does not come out correctly from the approximate analysis.

Let us look now at the overlap distribution $\pi(s)$ shown in Fig. 4a for $t = 2^k$, $k = 6,..., 9$. The distribution is peaked at both ends, $s = 0$ for no overlap and $s = t$ for full overlap, with $\pi_t(0) \simeq 0.28$ and $\pi_t(t) \simeq 0.23$ as $t \to \infty$. In the neighborhood of the two peaks, there is a power-law decay $\pi_t(s) \sim s^{-3/2}$ and $\pi_t(t-s) \sim s^{-3/2}$, $s \ll t$. While the distribution tends to a limiting form at both ends, the center part decreases with increasing t. In Fig. 4b we plot $t^{3/2}\pi_t(s)$ against the fractional overlap $q = s/t$, using the same set of data as in Fig. 4a. The collapse of the curves indicates that, except for $s = 0$ or t, the distribution at large t obeys scaling

$$\pi_t(s) \simeq t^{-3/2}\, \hat{\pi}(s/t) \tag{3.5}$$

where $\hat{\pi}(x)$, $\hat{\pi}(1-x) \sim x^{-3/2}$ for $x \ll 1$. In the limit $t \to \infty$, $P_{\text{ovp}}(q) \equiv t\pi_t(qt)$ approaches a sum of two δ-functions at $q = 0$ and $q = 1$. This result is in agreement with that of ref. 5.

3.2. Hard-Core Repulsion

Another limiting case is that of hard-core repulsion between the two lines. In this case the minimum in Eq. (2.4b) is given by the last term on the right-hand-side,

$$E_t^{(2)} = E_{t-1}^{(1)} + \varepsilon + E_{t-1}^{\prime(1)} + \varepsilon' \tag{3.6}$$

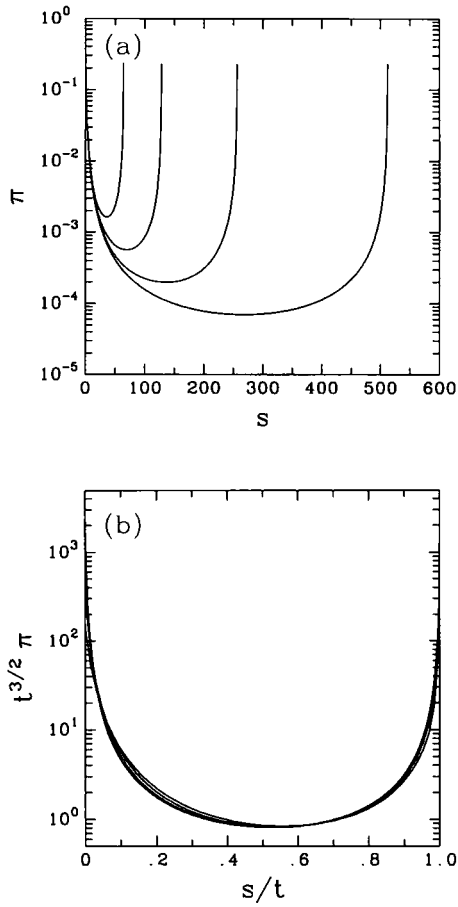

Fig. 4. (a) Distribution of the overlap in the ground state of a single line on the Cayley tree. Here $t = 64$, 128, 256, and 512 (from left to right). (b) A scaling plot of the data shown in (a).

Using (2.4a) and (3.6), we easily verify the following expression for the interaction energy $E_{\text{int},t} = E_t^{(2)} - 2E_t^{(1)}$ in the ground state:

$$E_{\text{int},t} = |E_{t-1}^{(1)} + \varepsilon - E_{t-1}'^{(1)} - \varepsilon'| \tag{3.7}$$

For the model defined by (2.18), E_{int} takes only nonnegative integer values. Let $\Psi_{\text{int}}(i)$ be the probability that $E_{\text{int}} = i$. For $i = 0$, $\Psi_{\text{int}}(0)$ is simply given by $\pi(0)$, the probability that the energy of the two branches is degenerate. On the other hand, $\Psi_{\text{int}}(i > 0)$ is twice the probability that the energy of

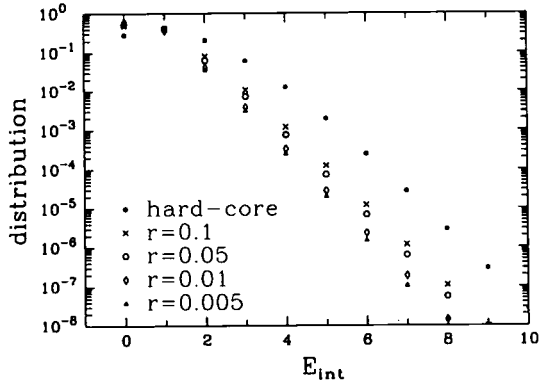

Fig. 5. Distribution of the interaction energy for two lines on the Cayley tree at large t.

one branch is i units higher than the energy of the other branch. Thus we have

$$\Psi_{\text{int},t}(0) = \sum_j [\hat{Q}_t(j) - \hat{Q}_t(j+1)]^2 \tag{3.8a}$$

$$\Psi_{\text{int},t}(i) = 2\sum_j [\hat{Q}_t(j) - \hat{Q}_t(j+1)][\hat{Q}_t(j+i) + \hat{Q}_t(j+1+u)] \tag{3.8b}$$

where $\hat{Q}_t(i) \equiv \hat{Q}_t(i;0)$ is given by a discretized version of (2.14a). Note the factor 2 difference between (3.8a) and (3.8b).

From Eq. (3.6) it is easy to see that, as $t \to \infty$,

$$\langle E_{\text{int}} \rangle = 2(\langle \varepsilon \rangle - e_0) = 2(p - e_0) \tag{3.9}$$

At $p = 0.8$, $\langle E_{\text{int}} \rangle \simeq 1.094$, in agreement with direct measurement. The distribution of E_{int} at large t is shown in Fig. 5 (full circles), together with those for weak repulsion discussed below.

3.3. Weak Repulsion

Consider now the model defined by Eqs. (2.18) and (2.19) at small r. For two lines sharing a path up to a distance s from the root O, the mean interaction energy is rs. By considering a configuration where both lines are in the one-line ground state, we obtain an upper bound for the interaction energy,

$$\langle E_{\text{int},t} \rangle \leqslant r \sum_{s=0}^{t} s\pi_t(s) \tag{3.10}$$

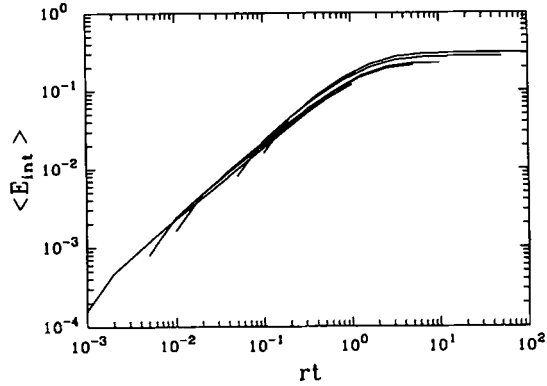

Fig. 6. Average interaction energy of two lines on the Cayley tree at weak repulsion. Each curve corresponds to a given value of the interaction strength r.

Here π_t is the overlap distribution for zero interaction as discussed in Section 3.1.

Since the sum in (3.10) is dominated by those at s close to t, we expect a linear increase of the interaction energy with t for $rt < 1$. When rs becomes of order 1 or larger, it is more favorable for one or both lines to get out of their ground state and seek one which has a smaller overlap, thus a smaller interaction energy. Figure 6 shows the mean interaction energy $\langle E_{\text{int}} \rangle$ against rt for $r = 0.001$, 0.005, 0.01, 0.05, and 0.1. The data collapse suggests a scaling form,

$$\langle E_{\text{int},t} \rangle \simeq \Phi_{\text{cay}}(rt) \tag{3.11}$$

where $\Phi_{\text{cay}}(x) \sim x$ for $x \ll 1$ and $\Phi_{\text{cay}}(x) \sim \text{const}$ for $x \gg 1$. The plateau part of the curves at large t does not collapse completely. This can be attributed to the finite probability for small overlaps. Since $\pi(s)$ decays as $s^{-3/2}$ for small s, the sum in (3.10) up to $s \simeq 1/r$ yields the following expression for the interaction energy at large t when r is small:

$$\langle E_{\text{int},\infty} \rangle \simeq e_1 + e_2 r^{1/2} \tag{3.12}$$

From our data we determined $e_1 \simeq 0.19$ and $e_2 \simeq 0.37$ at $p = 0.8$.

The distribution of the interaction energy at large t is shown in Fig. 5 for a set of r values. It appears that there is a limiting form as $r \to 0$.

4. HIERARCHICAL LATTICES

4.1. Noninteracting Lines

Compared to the situation on Cayley tree, our knowledge on the properties of the ground state of a single line on a disordered hierarchical lattice is mainly numerical, although a perturbative scheme for b close to 1 has been developed by Derrida and Griffiths[14] to provide some analytical insight. The general picture[14,16,17] may be summarized as follows.

(i) As the generation k of the lattice increases, the distribution of the ground-state energy $E^{(1)}$, in our notation $-\partial \hat{P}_k(x)/\partial x$, tends to a scaling form,

$$-\frac{\partial \hat{P}_k(x)}{\partial x} \simeq \delta_k^{-1} F_b\left(\frac{x-\gamma_k}{\delta_k}\right) \tag{4.1}$$

where $\gamma_k = \langle E_k^{(1)} \rangle$ and $\delta_k^2 = \langle (E_k^{(1)})^2 \rangle - \langle E_k^{(1)} \rangle^2$. The scaling function $F_b(x)$ is independent of the distribution $\rho_\varepsilon(x)$ of random energies ε, provided $\rho_\varepsilon(x)$ decays to zero sufficiently fast as $x \to -\infty$. (This is in contrast to the behavior on the Cayley tree, where W is not uninversal. It can be understood from the fact that here ρ_ε does not enter the recursion relations explicitly.) The root-mean-square fluctuation of the ground-state energy δ_k grows as a power law of the length $t = 2^k$,

$$\delta_k \sim t^\omega \tag{4.2}$$

where $\omega(b)$ is a monotonically decreasing function of b, starting at $\omega(1) = 1/2$.

(ii) Cook and Derrida[16] studied the overlap distribution at a finite temperature, and found only a single peak whose position depends on temperature, suggesting absence of nontrivial ground-state degeneracy.

In the following we present results obtained from the iteration of Eqs. (2.16) and (2.17) for $b = 2$, 4, and 8. The mean ground-state energy is generally found to take the form

$$\gamma_k = e_0 t + c_1 \delta_k + O(1) \tag{4.3}$$

where $c_1(b)$ is a universal amplitude ratio which depends only on the branch number b. Values of c_1 for $b = 2$, 4, and 8 are listed in Table I, along with $\omega(b)$.

In Fig. 7 we plot the overlap distribution $P_{ovp}(q, t) \equiv t\pi(qt)$ for $b = 2$, $p = 0.8$, and $t = 128, \ldots, 2048$. The probability density has two main peaks,

Table I. Energy Fluctuation Exponent ω and Scaling Amplitudes on the Hierarchical Lattice

b	ω	c_1	c_2
2	0.2988	1.033	1.155
4	0.205	1.77	0.94
8	0.156	2.45	0.9

one at $q=0$, the other at $q=q_1$, $q_1 \simeq 0.45$. The peak at $q=0$ contains only a single point $s=0$, with

$$P_{\text{ovp}}(0, t) \sim t^{1-\omega} \tag{4.4}$$

The peak at $q=q_1$ has a width $\delta q \sim t^{-\omega}$ and an amplitude proportional to t^{ω}. This peak tends to a delta function as $t \to \infty$. In addition, there is a set of minor peaks located at $q_i \simeq q_1/2^{i-1}$, $i=2, 3,...$, etc., which arise naturally in the iteration process as combinations of the two major peaks. These peaks are expected to have vanishing weight in the limit $t \to \infty$.

The behavior of the overlap distribution appears to be similar at $b=4$ and $b=8$, although the secondary peaks are more pronounced than in the $b=2$ case.

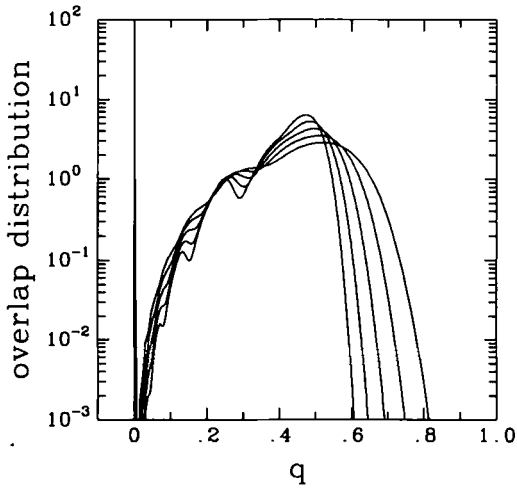

Fig. 7. Distribution of the overlap in the ground state of a single line on the hierarchical lattice at $b=2$, $p=0.8$, and $t=128$, 256, 512, 1024, and 2048 (from right to left at the right tail). The peak around $q \simeq 0.45$ sharpens as t increases.

4.2. Hard-Core Repulsion

We now turn to the case of two lines with a hard-core repulsion on the hierarchical lattice. Even though the two lines are not allowed to occupy the same bond, they may still be on the same branch, in contrast to the case on the Cayley tree. Figure 8a shows the probability distribution $\Psi_{\text{int}}(E_{\text{int}})$ for the interaction energy $E_{\text{int}} = E^{(2)} - 2E^{(1)}$. As before, $\Psi_{\text{int}}(0)$ is given by the probability $\pi(0)$ for zero overlap of noninteracting lines, and hence decreases as $t^{-\omega}$. The peak of the distribution moves to the right

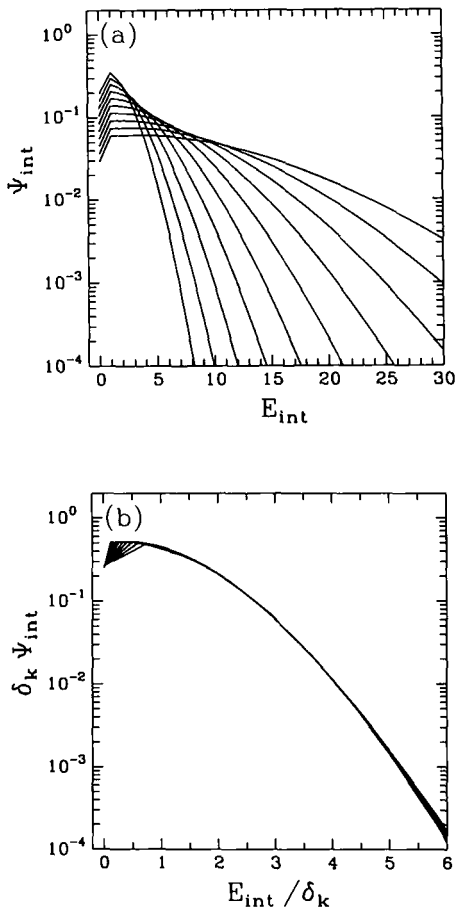

Fig. 8. (a) Distribution of the interaction energy for two lines on the hierarchical lattice at $b = 2$ and with hard-core repulsion. From bottom left to right, t increases in successive powers of 2 starting from $t = 32$. (b) Scaling plot of (a).

as t^{ω}. Figure 8b shows a scaling plot of the data. The data collapse suggests the scaling form

$$\Psi_{\text{int},k}(i) = \delta_k^{-1} G_b(i/\delta_k) \tag{4.5}$$

where δ_k is defined through (4.1). Note that $G_b(x)$ tends to a finite value as $x \to 0$, though $\Psi_{\text{int},k}(0)$ seems to be smaller by a factor 2 than $\Psi_{\text{int},k}(1)$ at large k. Similar behavior is found for $b = 4$ and 8.

From Eq. (4.5) for the distribution we conclude that the mean interaction energy should be proportional to δ_k,

$$\langle E_{\text{int},k} \rangle \simeq c_2 \delta_k \tag{4.6}$$

An upper bound on $\langle E_{\text{int},k} \rangle$ can be obtained by restricting the two lines to two (given) different branches. The mean energy of the latter arrangement is given by $4\gamma_{k-1}$. Using Eqs. (4.3) and (4.6), we obtain, for $b \geqslant 2$,

$$c_2 \leqslant 2(2^{1-\omega} - 1) c_1 \tag{4.7}$$

From our data for $\langle E_{\text{int},k} \rangle$ we have determined c_2 for $b = 2$, 4 and 8, as given in Table I. The inequality (4.7) is indeed satisfied.

4.3. Weak Repulsion

The inequality (3.10) holds also on the hierarchical lattice. Since the typical fractional overlap in the ground state of one line is finite (see Fig. 7), at small values of rt, we expect a linear increase of the interaction energy with the length of the line t. Another upper bound on the interaction energy is given by that of hard-core repulsion, Eq. (4.6). A crossover is thus expected at $rt \simeq \delta_k$. Figure 9 shows scaled data for the mean interaction energy against t for $b = 2$ and various r values. The data collapse confirms the scaling,

$$\langle E_{\text{int}} \rangle \simeq \delta_k \Phi_{\text{hir}}(rt/\delta_k) \tag{4.8}$$

where $\Phi_{\text{hir}}(x) \sim x$ for $x \ll 1$ and crosses over to c_2 at $x \gg 1$.

Figure 10 shows the distribution of the interaction energy at $r = 0.05$. It is seen that data for $rt \gg \delta_k$ become almost identical to those of hard-core repulsion. This property is observed to hold also for $b = 4$ and $b = 8$.

5. REPULSIVE LINES IN (1 + 1) DIMENSIONS

Our results on hierarchical lattices are in full agreement with the picture proposed earlier by Parisi[8] and Mézard[9] based on their investigation of the problem in (1 + 1) dimensions, and thus seems to imply

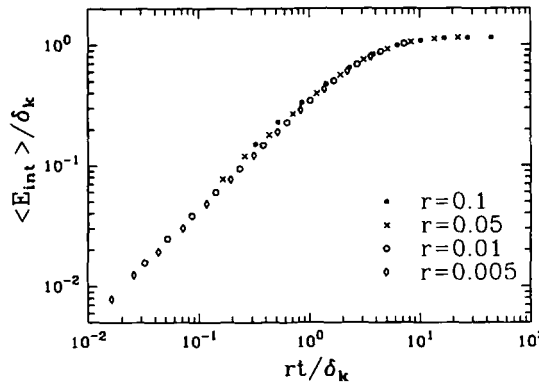

Fig. 9. Average interaction energy of two lines on the hierarchical lattice at $b = 2$. Weak repulsion.

that the behavior is quite general. There remains, however, a puzzling aspect. For simplicity, let us consider the $(1 + 1)$-dimensional case with an energy functional (1.2a). The lower end of the line is in contact with a "substrate" at $t = 0$, but is free to move in the transverse direction. The ground-state energy $E(x, t)$ of the line is then a function of the upper end coordinates (x, t). The ground-state line configurations at different values of x form tree structures,[6,18] with roots at $t = 0$. The lateral span of one tree is of the order of t^{ζ}, where $\zeta = 2/3$ is the roughness exponent of the line.

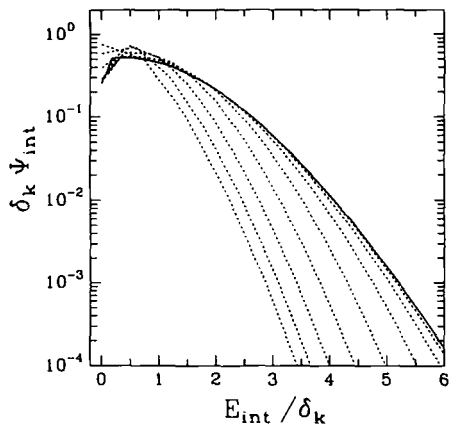

Fig. 10. Distribution of the interaction energy of two lines on the hierarchical lattice at $b = 2$ and $r = 0.05$ (dashed lines). From bottom left to right, t increases in successive powers of 2 starting from $t = 32$. Solid line shows the same data for hard-core repulsion at $t = 4096$.

When x is at the border between two neighboring trees, there are two degenerate, nonoverlapping ground-state configurations. The probability for such a situation is inversely proportional to the lateral span of the tree, i.e., of the order of $t^{-\zeta}$, much less than the value $t^{-\omega}$ suggested by Mézard and Parisi!

We have performed Monte Carlo transfer matrix calculations on a lattice version of two directed lines in $(1+1)$ dimensions. The lines are put on a square lattice tilted by 45 deg. At each point a line can go either up-left or up-right, and picks up a random site energy ε which takes value 1 with probability p and 0 with probability $1-p$. For hard-core repulsion, which is the only case considered here, two lines are allowed to visit the same site but not to share the same bond. In Fig. 11 we plot the probabilities $\Psi_{\text{int},t}(i)$, $i=0, 1, 2$, for the interaction energy $E_{\text{int}} = E^{(2)} - 2E^{(1)} = i$ as a function of the length t. The data seem to confirm

$$\Psi_{\text{int},t}(0) \sim t^{-\zeta} \tag{5.1}$$

Figure 12 shows the full distribution $\Psi_{\text{int},t}(E_{\text{int}})$ at $p=0.8$ in scaled form. Apart from $E_{\text{int}}=0$, there is a good data collapse, yielding

$$\Psi_{\text{int},t}(E_{\text{int}}) \simeq \delta_t^{-1} G_{(1+1)}(E_{\text{int}}/\delta_t) \tag{5.2}$$

where δ_t is the root-mean-square deviation of the one-line ground-state energy. In contrast to the behavior on the hierarchical lattice, the scaling function $G_{(1+1)}(x)$ appears to approach zero linearly with x at small x. Nevertheless, the mean value of the interaction energy is still proportional to δ_t, with $c_2 = \langle E_{\text{int}} \rangle / \delta_t \simeq 1.6$.

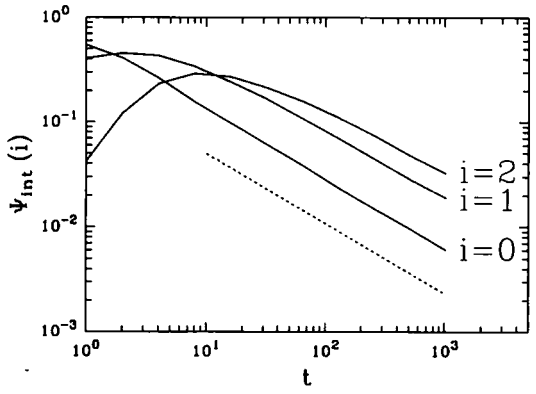

Fig. 11. Two lines in $(1+1)$ dimensions with hard-core repulsion. Solid lines give the probabilities for the interaction energy to be equal to 0, 1, and 2 as a function of the length t. Dashed line indicates a power-law behavior with an exponent $-2/3$.

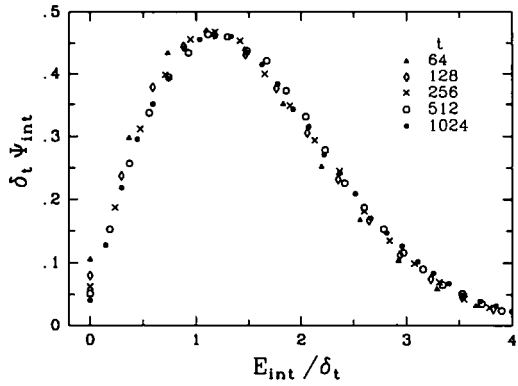

Fig. 12. Scaled form for the distribution of the interaction energy for two lines in $(1+1)$ dimensions with a hard-core repulsion.

Mézard[9] has shown that, with one end of the line fixed at a given point, thermal fluctuations in the position of the other end are proportional to the length of the line. (This property is a direct consequence of Galilean invariance for the corresponding Burgers equation.[19,20]) With the assumption that the probability for the occurrence of almost degenerate yet non-overlapping states is of the order of $t^{-\omega}$, this result is readily explained. Such an interpretation is, however, in seeming contradiction with (5.1).

6. CONCLUSIONS

The main finding of the present paper may be summarized as follows.

(i) *Degenerate ground state of a single line.* We performed explicit calculations of the overlap distribution $P_{ovp}(q)$ for degenerate ground-state configurations and studied its scaling behavior with respect to the length t. The results confirm those of earlier studies: on the Cayley tree, $P_{ovp}(q)$ approaches a sum of two delta functions at $q=0$ (no overlap) and $q=1$ (full overlap) in the limit $t \to \infty$; on the hierarchical lattice, $P_{ovp}(q)$ approaches a single delta function at $q=q_1$ $(0<q_1<1)$ in this limit, but there is a probability of order $t^{-\omega}$ for no overlap, where ω is the energy fluctuation exponent. Our finding for a model with discrete bond energies should apply to those with a continuous distribution of bond energies (properly bounded at the lower end) if we replace the term "degeneracy" by "near-degeneracy" in the discussion.

(ii) *Two repulsive lines with one or both ends fixed at the same position.* The excess energy E_{int} of the two-line system grows as the ground-state

energy fluctuation t^{ω} of a single line, in the limit $t \to \infty$. When the strength of the interaction r is weak, there is a crossover from a linear behavior $E_{\text{int}} \simeq rt$ for small t to the asymptotic behavior $E_{\text{int}} \sim t^{\omega}$ at large t. This crossover is also reflected in the ground-state configuration of the two lines: for $rt \ll t^{\omega}$ they (on the hierarchical lattice) typically form a bound state in the same deep valley of the one-line energy landscape; for $rt \gg t^{\omega}$ the two lines are driven to different valleys, in which case the strength of the interaction is no longer relevant. On the hierarchical lattice, this picture is confirmed by our direct computation of the probability for no overlap (not presented here), which follows the behavior at $r = 0$ initially but crosses over to 1 at large t. The distribution of the interaction energy also approaches an r-independent form (4.5) in the large-t limit.

(iii) *A discrepancy in* $(1+1)$ *dimensions.* Although the general picture of multiple-valley energy landscape and of the crossover from bound to nonoverlapping states at weak repulsion is expected to carry over to finite-dimensional lattices, there seems to be a discrepancy in the probability for (almost) degeneracy of two nonoverlapping valleys. On the hiearchical lattice this probability decreases as $t^{-\omega}$, while our Monte Carlo transfer matrix calculations in $(1+1)$ dimensions indicate that the probability should decrease much faster with t, in fact as $t^{-\zeta}$, where ζ is the roughness exponent of the line. If this is true, further work is needed to understand thermal fluctuations of the transverse end-to-end displacement of one line.

The ground-state properties of the two-line system studied here should be relevant to the thermodynamic behavior of a type II superconductor with disorder close to the lower critical field H_{c1}.[1-4] In particular, the scaling behavior of the interaction energy E_{int} with the length t determines how the equilibrium density of flux lines varies with the external magnetic field H close to H_{c1}. Our finding that, for hard-core repulsion, E_{int} increases as t^{ω} confirms an earlier prediction by Nattermann and Lipowsky.[2] The renormalization group (RG) analysis of ref. 3 arrived at a different conclusion for $d > 2$ (including the physical dimension $d = 3$). It would be interesting to explore whether this discrepancy is due to an insufficient set of parameters considered in the RG analysis or is a result of replica symmetry breaking for the two-line system.

APPENDIX

In this appendix we present an approximate calculation on the Cayley tree for the one-line ground-state energy and its distribution. On the tree,

a path is uniquely determined by its end coordinate i, $i = 1, 2, ..., 2^t$. The energy of the path is thus given by

$$E(i) = \sum_{j=1}^{t} \varepsilon_j(i) \tag{A1}$$

For the model specified by (2.18), $E(i)$ obeys a binary distribution,

$$\Psi_E(m) = C_t^m p^m (1-p)^{t-m} \tag{A2}$$

From (A2) we obtain

$$\langle E(i) \rangle = pt, \qquad \langle E(i)^2 \rangle - \langle E(i) \rangle^2 = p(1-p)t \tag{A3}$$

The ground-state energy $E_t^{(1)}$ is given by the minimum of the 2^t energies $E(i)$. If we assume that these energies are independent realizations of (A2), we arrive at the following approximate expression for the probability that $E_t^{(1)} \geqslant m$:

$$\hat{P}_t(m) \simeq \left[1 - \sum_{n=0}^{m-1} \Psi_E(n)\right]^{2^t} \simeq \exp\left[-2^t \sum_{n=0}^{m-1} \Psi_E(n)\right] \tag{A4}$$

To put $\hat{P}_t(m)$ in the traveling-wave form (3.1), we consider the following integral representation for Ψ_E:

$$\Psi_E(n) = \frac{1}{2\pi i} \oint_S \frac{dz}{z^{n+1}} (1 - p + zp)^t \tag{A5}$$

where S is any closed contour on the complex z-plane enclosing the origin. Substituting (A5) into (A4) and carrying out the sum over n, we obtain

$$\hat{P}_t(m) \simeq \exp[-2^t I_t(m)] \tag{A6}$$

where

$$I_t(m) = \frac{1}{2\pi i} \oint_S dz \frac{1 - z^{-m}}{z - 1} (1 - p + zp)^t \tag{A7}$$

For m, $t \gg 1$, the integral can be evaluated using the method of steepest descent and the result is given by, for $m < pt$,

$$I_t(m) \simeq A_p(m/t) \exp[-t f_p(m/t) - \tfrac{1}{2} \ln t] \tag{A8}$$

where

$$A_p(x) = \frac{1-p}{p-x} \left(\frac{x}{2\pi(1-x)}\right)^{1/2} \tag{A9}$$

$$f_p(x) = x \ln\left(\frac{x}{p}\right) + (1-x) \ln\left(\frac{1-x}{1-p}\right) \tag{A10}$$

From (A6) we see that the typical value of $E^{(1)}$ is at an m where $2^t I_t(m) \simeq 1$, i.e., the very tail of the distribution (A2). Let e_0 satisfy

$$f_p(e_0) = \ln 2 \tag{A11}$$

Expanding $f_p(x)$ around $x = e_0$ and keeping only the term linear in $x - e_0$, we obtain

$$2^t I_t(m) \simeq A(e_0) \exp[\psi(m - e_0 t - C' \ln t)] \tag{A12}$$

where

$$\psi = -f_p'(e_0) = \ln\left[\frac{p(1-e_0)}{e_0(1-p)}\right] \tag{A13}$$

and $C' = 1/(2\psi)$. Substituting (A12) into (A6) yields (3.1).

NOTE ADDED IN PROOF

The connection between the directed polymer problem on the Cayley tree and the random energy model, as discussed in the appendix, was noted earlier by J. Cook and B. Derrida, *J. Stat. Phys.* **63**:505 (1991).

ACKNOWLEDGMENTS

I wish to thank T. Hwa and T. Nattermann for enlightening conversations. This work is supported in part by the German Science Foundation under project SFB 341.

REFERENCES

1. D. R. Nelson, *Phys. Rev. Lett.* **60**:1973 (1988); D. R. Nelson and P. Le Doussal, *Phys. Rev. B* **42**:10113 (1990).
2. T. Nattermann and R. Lipowsky, *Phys. Rev. Lett.* **61**:2508 (1988).
3. T. Natterman, M. Feigelman, and I. Lyuksyutov, *Z. Phys. B* **84**:353 (1991).
4. D. S. Fisher, M. P. A. Fisher, and D. A. Huse, *Phys. Rev. B* **43**:130 (1991); D. J. Bishop, P. L. Gammel, D. A. Huse, and C. A. Murray, *Science* **255**:165 (1992); and references therein.
5. B. Derrida and H. Spohn, *J. Stat. Phys.* **51**:817 (1988).
6. M. Kardar and Y.-C. Zhang, *Phys. Rev. Lett.* **58**:2087 (1987).
7. M. Kadar, *Nucl. Phys. B* **290**:582 (1987).
8. G. Parisi, *J. Phys.* (Paris) **51**:1595 (1990).
9. M. Mézard, *J. Phys.* (Paris) **51**:1831 (1990).
10. D. S. Fisher and D. A. Huse, *Phys. Rev. B* **43**:10728 (1991).
11. L.-H. Tang and I. F. Lyuksyutov, *Phys. Rev. Lett.* **71**:2745 (1993).
12. L. Balents and M. Kardar, *Europhys. Lett.* **23**:503 (1993).

13. T. Hwa and T. Nattermann, to be published.
14. B. Derrida and R. B. Griffiths, *Europhys. Lett.* **8**:111 (1989).
15. A. N. Berker and S. Ostlund, *J. Phys. C* **12**:4961 (1981).
16. J. Cook and B. Derrida, *J. Stat. Phys.* **57**:89 (1989).
17. T. Halpin-Healy, *Phys. Rev. A* **42**:711 (1990).
18. L.-H. Tang, J. Kertész, and D. E. Wolf, *J. Phys. A* **24**:L1193 (1991).
19. D. A. Huse, C. L. Henley, and D. S. Fisher, *Phys. Rev. Lett.* **55**:2924 (1985).
20. E. Medina, T. Hwa, M. Kardar, and Y.-C. Zhang, *Phys. Rev. A* **39**:3053 (1989).